Modern Physics Letters B, Vol. 24, No. 2 (2010) 151–160

DOI: 10.1142/S0217984910022330

World Scientific
www.worldscientific.com

SYNTHESIS AND OPTICAL PROPERTIES OF LARGE-SCALE ALIGNED ALUMINA NANOWIRE ARRAYS

JIE XU, WEI LIU, GUO-AN CHENG* and RUI-TING ZHENG

Key Laboratory of Beam Technology and Material Modification of Ministry of Education, College of Nuclear Science and Technology, Beijing Normal University, Beijing 100875, China
**gacheng@bnu.edu.cn*

Received 8 April 2009
Revised 27 August 2009

Ordered large-scale alumina nanowire arrays on the surface of porous anodic alumina membranes (AAMs) have been synthesized by chemical etching. The analysis shows that amorphous alumina nanowires directly formed from AAMs have uniform size and shape. The mean length and mean diameter of alumina nanowires are about 6 μm and 24 nm, respectively. It is observed that chemical etching parameters affect the synthesis of alumina nanowires and preferable experimental conditions for the synthesis of alumina nanowire arrays. The intensity of photoluminescence excited from alumina nanowire is affected by post-annealing temperatures. The mechanisms for the synthesis and PL emission of alumina nanowires are discussed.

Keywords: Anodic alumina; porous membrane; alumina nanowire; photoluminescence.

1. Introduction

Since the successful synthesis of the carbon nanotube, one-dimensional materials have stimulated great interest due to their peculiar structures and unique properties as well as potential applications in magnetic,[1] optical,[2,3] electronic[4] and micromechanical devices.[5] In order to realize the most potential applications, it is quite important and necessary to synthesize large-scale and highly oriented nanostructures. In the fabrication of nanomaterials, much effort has been focused on template synthesis methods.[6–9] Among them, a self-ordered nanochannel structure synthesized by anodizing high purity aluminum foils in an appropriate acid solution has became a key template due to their particular characteristics such as controllable pore diameter, high aspect ratio of channels and periodic distribution.

Alumina nanowires (ANWs) have been fabricated in several ways in the past, such as thermal evaporation of alumina and aluminum powders[10]; *in situ* catalytic

*Corresponding author.

growth of ANWs by heating a mixture of SiO_2, Al and Fe_2O_3 catalyst[11]; electrodeposition in the nanochannels of AAMs[12]; Kuiry *et al.* used sol–gel method to fabricate ANWs[13]; Mei *et al.* detached ANWs from Si-based AAMs[14]; Li *et al.* synthesized alumina nanorods using an arc-discharge method.[15–17] These methods employ both a high temperature and strict fabrication process. The chemical etching method provides an efficient and rational approach for large-scale and low-cost alumina nanostructures for realistic application in nanoscience. In this article, we report a facile method to fabricate pure and oriented ANWs by etching as-prepared AAMs in phosphoric acid solution. The PL properties of ANWs are investigated.

2. Experiment

AAMs as the precursor of ANWs synthesis were prepared via two-step anodization. All chemicals were of analytical grade reagents and used as-received without further purification. An aluminum sheet with a purity of 99.999% was cut into small pieces of about 3×3 cm. These small specimens were first degreased in acetone with ultrasonic vibration, followed by annealing at 550°C in a nitrogen atmosphere furnace for 3 h. The specimens were then chemical polished in a mixture solution of phosphoric acid, sulfuric acid and nitric acid (with a volume ratio of 5:4:1) for 2 min to further remove surface impurities. After these pretreatments, the specimens were anodized in a 0.3 M oxalic acid aqueous solution under the anodic oxidization voltage of 40 V for 30 min at room temperature. The anodic oxide layer on the surface of AAM was then removed using a mixed solution of phosphoric acid (6 wt.%) and chromic acid (1.8 wt.%). Afterwards, the second anodization was carried out under the same condition as described in the first step for 1 h, and then the specimens were rinsed in deionized water several times. The ANWs were synthesized using chemical etching; phosphoric acid was selected as the etching solution. Different growth situations could be observed when the concentration of etching solution was changed from 4 wt.% to 12 wt.% under a certain reaction temperature. The growth situation was also recorded when the reaction temperature was adjusted from 20°C to 60°C while the concentration of etching solution was maintained at 8 wt.%. The post-annealing of ANWs was carried out at the temperature range from 250°C to 600°C for 3 h in air.

ANWs morphologies were observed by field emission scanning electron microscopy (FESEM; Hitach S-4800) and transmission electron microscopy (TEM; JEOL JEM-200CX). PL spectral measurements were taken using an ISA-USA fluorescence spectrometer (Fluorolog-Tau-3) with Xe lamp as the excitation light source, the spectral resolution was about 0.2 nm.

3. Results and Discussion

The surface morphology of the typical AAMs obtained in our experiment is shown in Fig. 1. It can be easily seen in Fig. 1(a) that the honeycomb structure has been fabricated and the cell arrangement is fairly ordered. The cross-section image of

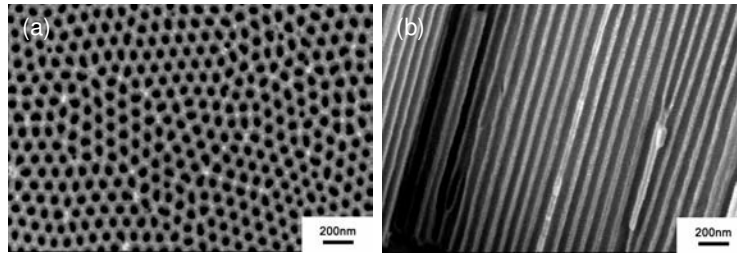

Fig. 1. SEM images of highly ordered anodic alumina membrane. (a) Top view morphology; (b) cross-section morphology.

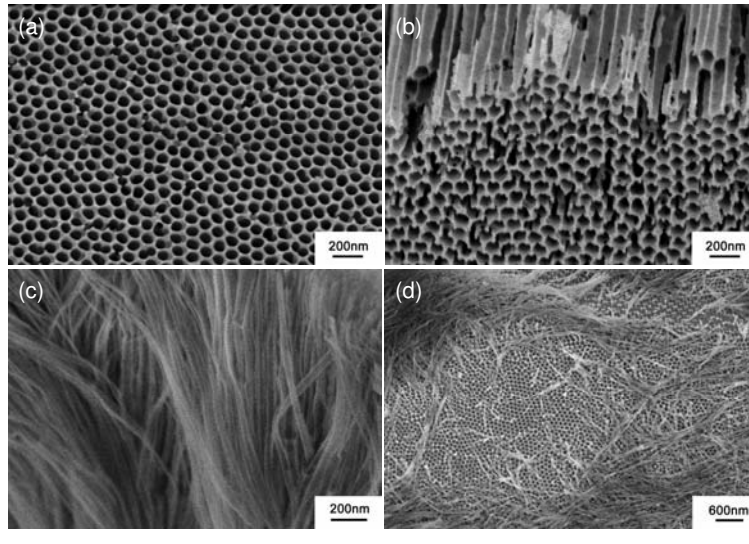

Fig. 2. SEM images of anodic alumina membrane etched in phosphoric acid solution for different times. (a) 10 min; (b) 12 min; (c) 14 min; (d) 17 min.

AAMs in Fig. 1(b) indicates that the inner surfaces of the nanochannels are very smooth and parallel to each other. The average diameter of pores and space between nanopores are about 56 nm and 100 nm, respectively. The average wall thickness between two neighboring pores is about 44 nm. This is a typical structure of AAMs as has been reported.[18,19]

The structure of AAMs will change when AAMs are put into a phosphoric acid solution for different etching durations. Figure 2 shows the SEM images of alumina nanostructures after AAMs had been etched in 8 wt.% phosphoric acid solution at 45°C for different durations. From Fig. 2(a), it is obvious that AAMs have the same honeycomb structure when chemical etching time is below 10 min. However, when the average diameter of the nanopores in the AAMs is increased to 90 nm and the thickness of the inter-wall between two neighoring pores etched into 10 nm, some

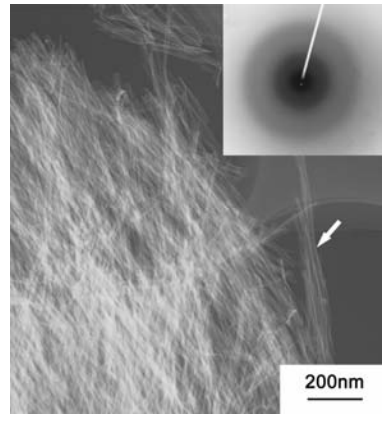

Fig. 3. TEM image of ANWs synthesized by etching in phosphoric acid solution for 14 min. Inset: SAED pattern taken from ANWs showing some amorphous halo rings.

broken pores are observed. When chemical etching time is increased to 12 min, there are a lot of walls to be etched, only the residual alumina at triple-pore junctions still remain (seen Fig. 2(b)). From Fig. 2(c), it can be seen that ordered ANWs have been synthesized after chemical etching for 14 min. The average diameter and length of ANWs are about 24 nm and 6 μm respectively. The nanowires stand on each corner of the hexagonal arrays and there are about 210 ANWs per square micron. Nevertheless, the ANW array has disappeared, and only a few short ANWs lie down on the surface of the hexagonal alumina barrier layer when the etching time is prolonged to 17 min; most parts of ANWs have been etched out. Figure 3 is a TEM image of ANWs which have been synthesized by etching in 8 wt.% phosphoric acid solution at 45°C for 14 min. A bundle of ANWs are observed on the Cu grid, with the average diameter of specimens about 25 nm, which is consistent with the result from Fig. 2(c). It is worth noting that the diameter of each ANW is not exactly the same, but distributed within a small range around 25 nm due to the inhomogeneity of the chemical etching process. The inset of Fig. 3 is a SAED pattern, and shows some amorphous halo rings. This indicates that ANWs are amorphous alumina.

From the above description, it can be seen that well oriented ANW arrays can be synthesized using AAMs. But the existing time of an ANW array is short. This means that the synthesis of ANWs is controlled by chemical etching parameters. In order to understand the growth situation of ANW arrays, the influence of chemical etching parameters on the synthesis of ANW arrays have been analyzed. These parameters include phosphoric acid concentration, etching time and solution temperature. Figure 4 shows the curves between the chemical etching time and length of ANWs under different phosphoric acid solution concentrations and different temperatures. The length of ANWs quickly increases with the increase of etching time in the first step, and reaches maximum length gradually. ANWs are then quickly etched out in the second step. A similar phenomenon is observed from Fig. 4(a).

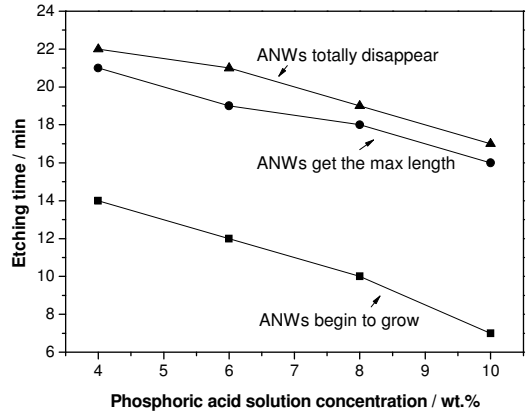

(a)

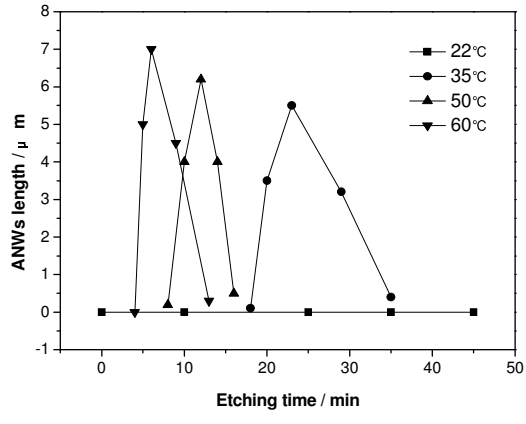

(b)

Fig. 4. Curves corresponding to the ANW synthesizing process. (a) Etching process under different phosphoric acid solution concentrations at 45°C; (b) etching process under different temperatures with 8 wt.% phosphoric acid solution.

Due to the increase of solution concentration, the ANW's transforming point will shift to an early time. But the existing time of ANWs are almost the same, approximately 9 minutes. The maximum length of ANWs are about 6–7 μm during the chemical etching process under a higher solution concentration, and gradually minimized with the decrease of solution concentration. This means that ANWs can be synthesized during the chemical etching at 45°C whether the solution concentration have been changed or not, but in order to get a proper nanowire length, the optimal phosphoric acid concentration must be in the range of 8 wt.% to 10 wt.%. However, ANWs cannot be synthesized if the solution temperature is lower than 22°C, and the curves gradually shift to the left with the increase of the solution temperature as described in Fig. 4(b). During the chemical etching process, the

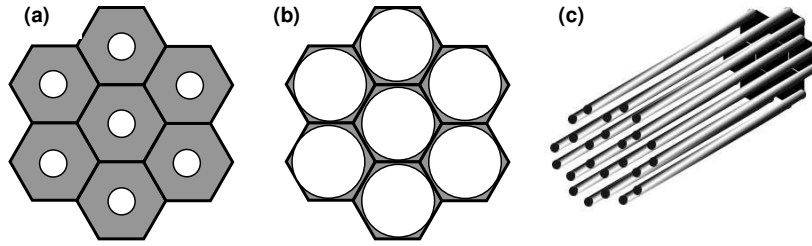

Fig. 5. A schematic representation of the formation of ANWs. (a) Porous alumina membrane; (b) pore-widening process; (c) alumina nanowires.

ANW's existing time is about 17 min at 35°C, but only about 8 min at 60°C. This indicates that both higher or lower solution temperatures will harm ANW synthesis, and the proper solution temperature is in the range of 40°C to 45°C. Figure 5 is a schematic illustration of the ANW formation process. The hexagonal cells are large-scale arrayed like a honey comb, as shown in Fig. 5(a). During the two-step anodization process, there are mainly three chemical reactions. They are as follows:

$$\text{Oxalic acid ionizing equation: } C_2H_2O_4 \rightarrow H^+ + HC_2O_4^-,$$

$$\text{Anode: } 2Al + 6OH^- \rightarrow Al_2O_3 + 3H_2O,$$

$$\text{Cathode: } 2H^+ \rightarrow H_2\uparrow.$$

Oxalic acid first ionized H^+ ions and the solution will generate OH^- ions to balance the charge. Hydroxyl groups move to anode position under the effect of electric field and react with aluminum; some aluminum will be oxidized into alumina. H^+ ions will assemble in the cathode position and transfer into hydrogen at the same time. Porous AAMs could be synthesized in this process, with the average increasing rate of thickness about 7 μm/h.

When the AAMs are immersed in the phosphoric acid solution, the phosphoric acid will ionize many H^+ ions. They react with alumina membrane fiercely.

$$Al_2O_3 + 6H^+ \rightarrow 2Al^{3+} + 3H_2O,$$

$$2Al + 6OH^- \rightarrow Al_2O_3 + 3H_2O.$$

Since the surface of the inner pore wall has a bigger reaction area, H^+ ions will react with the inner side of the alumina membrane more strongly, thus widening the pore diameter during the reaction, as shown in Fig. 5(b). The OH^- ions will be neutralized partly, and little would reach the bottom of the membrane to synthesize more alumina structures. That means the second equation would hardly happen here. In our experiment, the average chemical etching rate is about 3.4 nm/min.

When the diameter of pores are widened sufficiently, the wall between two neighoring pores will break; only the pillar shape alumina in the triple point position will remain. As the reaction process continues, the brims of the pillar alumina will be etched away, and the final round alumina nanowires fabricated.

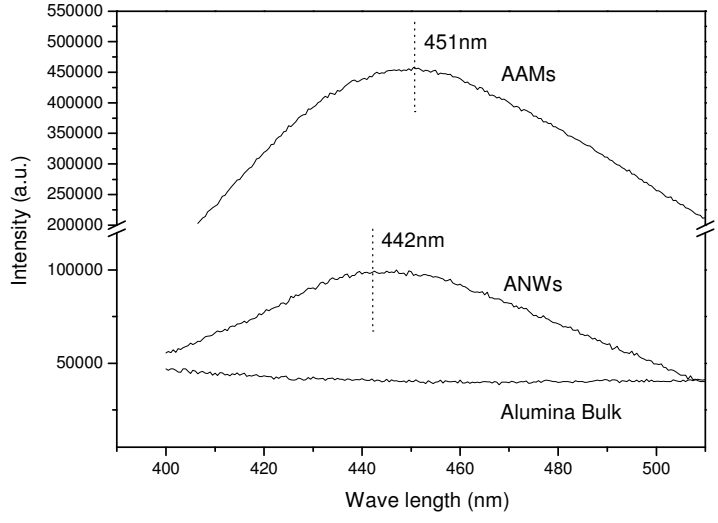

Fig. 6. PL spectra of the alumina bulks (alumina calcined in the air), AAMs and ANWs.

Figure 6 shows the photoluminescence (PL) spectra of bulk alumina, AAMs and ANWs, measured with an excitation of the 260 nm line of a Xe lamp. Bulk alumina is fabricated by heating aluminum at 500°C for 5 h in air. It is obvious that there is no apparent PL emission in bulk alumina. However, an intensive PL emission band at around 450 nm can be obtained in the AAM porous template. AAMs with porous structures are fabricated by anodizing in the oxalic acid, and composed with amorphous alumina. There are many luminescent centers to be formed during the anodizing process.[20,21] At the same time, a PL emission band is observed in ANWs, which have been synthesized using AAM template. The intensity of PL emission is obviously lower than that in the AAM template, and the position of PL peak has shifted from 451 to 442 nm. This indicates that the ratio of luminescent centers changed during the chemical etching.

The PL properties of ANWs post-annealed at different temperatures are also investigated. Figure 7 shows the PL spectra of ANWs post-annealed at different temperatures, which have also been measured with an excitation wavelength of 260 nm of a Xe lamp. It can be seen in Fig. 7 that the intensity of PL emission is first increased with the increase of post-annealing temperature, arriving at maximum value when the post-annealing temperature reaches 300°C. However, when the temperature is higher than 300°C, the intensity of PL emission drastically reduces as the post-annealing temperatures increase, nearly disappearing at temperatures higher than 600°C.

According to theoretical analysis reports, there are mainly two factors responsible for the PL emission in anodized alumina structures, such as oxygen vacancy (F^+) and oxalic acid radical impurities.[22,23] For bulk alumina from calcination in

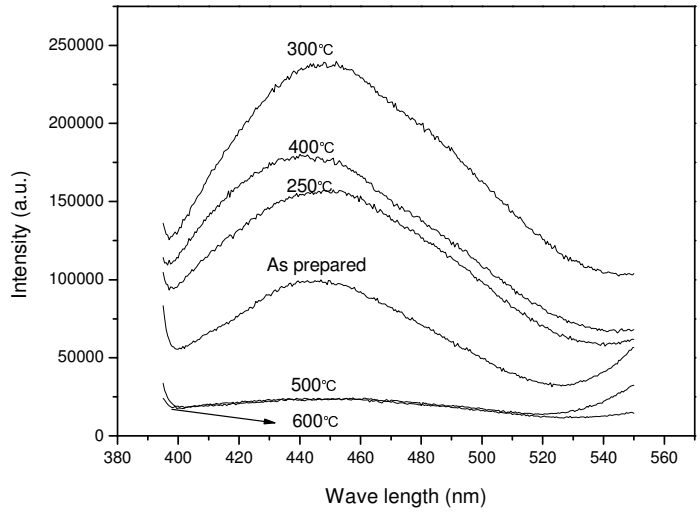

Fig. 7. PL spectra of the as-prepared ANWs and the ANWs annealed at different temperatures for 3 h in air.

the air, it has a perfect molecular structure and no defects (such as oxygen vacancy F^+, oxalic radical impurities, etc.) exist in alumina. This means that bulk alumina fabricated by calcination should never have any PL emissions. For alumina structures synthesized through anodic oxidization, the situation is completely different. Anodic oxidization is carried out in aqueous solution in which oxygen ions are relatively insufficient. This will induce some O^{2-} ions transform into O^- (F^+), which then become luminescent centers inside of the anodized alumina structure. On the other hand, the oxalic impurities will inevitable exist in alumina during anodic oxidization. Theoretical calculation indicates that the PL emission peak of F^+ is located at 400 nm and PL emission band of oxalic impurities is located around 470 nm. However, the PL emission peak located at 450 nm is obtained in anodized alumina structures in our experiment, and the width at half height of peak is about 70 nm. This indicates that the PL emission band has a composite peak, and proves that there are different luminescent centers existing in anodized alumina.

During the chemical etching process, the thin walls between nearby pores in AAMs corrode away and ANWs are synthesized. At this time, the oxygen environment is insufficient, which means that the trapped electron oxygen vacancy will exist in the new structure-ANWs. But as there is no more oxalic acid solution, and a great part of oxalic impurities in alumina dissolve into the aqueous solution, the process will certainly reduce the intensity of oxalic radical PL emission and make a blue-shift of PL emission peak as shown in Fig. 6.

When the annealing process is initially undertaken for several temperatures below 300°C, the aggregated oxygen vacancy (F^+) inside the ANWs slowly scatter off and F^+ amount increases at the same time. Since oxygen vacancy is one of

the most effective luminescent centers, the PL intensity increases. When the post-annealing temperature is higher than 300°C, the elevated temperature enhances diffusion of oxygen ions in ANWs and the stress-relief effect begins to appear. This means that the defects inside the ANWs slowly decrease. These integrated factors cause PL emission to disappear at the end.

4. Conclusion

In summary, we have successfully fabricated alumina nanowires from Al-based AAMs by chemical etching. The ANWs are around 24 nm in diameter and about 6 μm in length. The appropriate etching temperature is between 45–50°C, and the proper concentration of phosphoric etching acid is in the range of 8 wt.% to 10 wt.%. The oxygen vacancy (F^+) and oxalic impurities are the main luminescent centers of ANWs, with different proportions of these two constituents determining the PL emission behavior of the structure. F^+ induces the peak position to undergo a blue shift while the oxalic impurities cause a red shift. When the annealing temperature reaches Ta = 300°C, the PL emission gains the highest intensity. The formation process of ANWs is proposed.

Acknowledgments

This work is supported by the National Basic Research Program of China (Grant No. 2010CB832905), and partially by the National Natural Science Foundation of China (Grant No. 10575011) and the Key Project of Science and Technology of Education of China (Grant No. 108124).

References

1. Y. Q. Chang, D. B. Wang, X. H. Luo and D. P. Yu, *Appl. Phys. Lett.* **83** (2003) 4020.
2. D. P. Yu, Z. G. Bai, J. J. Wang and S. Q. Feng, *Phys. Rev. B* **59** (1999) 2498.
3. A. M. Morales and C. M. Lieber, *Science* **279** (1998) 208.
4. X. F. Duan, Y. Huang, Y. Cui and C. M. Lieber, *Nature* **409** (2001) 66.
5. Y. Cui and C. M. Lieber, *Science* **291** (2001) 851.
6. Y. Li and G. W. Meng, *Appl. Phys. Lett.* **76** (2000) 2011.
7. D. Xu, *J. Phys. Chem.* **104** (2000) 5061.
8. T. Gao and G. W. Meng, *Appl. Phys. A* **73** (2001) 251–254.
9. J. Zhang and L. D. Zhang, *J. Phys. Chem.* **115** (2001) 5714.
10. Q. Zhao, X. Xu, H. Zhang and D. Yu, *Appl. Phys. A* **79** (2004) 1721.
11. J. Zhou, S. Z. Deng, J. Chen and N. S. Xu, *Chem. Phys. Lett.* **365** (2002) 505.
12. Y. T. Pang, G. W. Meng, L. D. Zhang and Y. Q. Mao, *J. Solid State Electrochem.* **7** (2003) 344.
13. S. C. Kuiry, E. Megen, S. D. Patil and S. Seal, *J. Phys. Chem. B* **109** (2005) 3868.
14. Y. F. Mei, X. L. Wu, X. F. Shao and G. G. Siu, *Phys. Lett. A* **309** (2003) 109.
15. W. F. Li, X. L. Ma, Y. Li, W. S. Zhang, W. Zhang and Z. D. Zhang, *Philos. Mag.* **85** (2005) 3809.
16. W. F. Li, X. L. Ma, W. S. Zhang, W. Zhang, Y. Li and Z. D. Zhang, *Phys. Status Solidi A* **203** (2006) 294.

17. W. F. Li, X. L. Ma and Y. Li, *J. Mater. Res.* **22** (2007) 595.
18. Y. T. Pang, G. W. Meng, L. D. Zhang and Y. Q. Mao, *J. Phys.: Condens. Matt.* **14** (2002) 11729.
19. X. J. Xu, G. T. Fei, L. Q. Zhu and X. W. Wang, *Mater. Lett.* **60** (2006) 2331–2334.
20. G. S. Huang, X. L. Wu, Y. F. Mei and G. G. Siu, *J. Appl. Phys.* **93** (2003) 582.
21. T. Gao, G. W. Meng and L. D. Zhang, *J. Phys.: Condens. Matt.* **15** (2003) 2071.
22. Y. Du, W. L. Cai, C. M. Mo and X. G. Zhu, *Appl. Phys. Lett.* **74** (1999) 2591.
23. W. L. Xu, M. J. Zheng, S. Wu and W. Z. Shen, *Appl. Phys. Lett.* **85** (2004) 4364.